

Transient heat transfer analysis of functionally graded CNT reinforced cylinders with various boundary conditions

Rasool Moradi-Dastjerdi¹ and Gholamhassan Payganeh^{*2}

¹ Young Researchers and Elite Club, Khomeinishahr Branch, Islamic Azad University, Khomeinishahr, Iran
² Department of Mechanical Engineering, Shahid Rajaee Teacher Training University (SRTTU), Tehran, Iran

(Received November 08, 2016, Revised April 05, 2017, Accepted April 11, 2017)

Abstract. In this work, transient heat transfer analysis of functionally graded (FG) carbon nanotube reinforced nanocomposite (CNTRC) cylinders with various essential and natural boundary conditions is investigated by a mesh-free method. The cylinders are subjected to thermal flux, convection environments and constant temperature faces. The material properties of the nanocomposite are estimated by an extended micro mechanical model in volume fraction form. The distribution of carbon nanotube (CNT) has a linear variation along the radial direction of axisymmetric cylinder. In the mesh-free analysis, moving least squares shape functions are used for approximation of temperature field in the weak form of heat transform equation and the transformation method is used for the imposition of essential boundary conditions. Newmark method is applied for solution time depended problem. The effects of CNT distribution pattern and volume fraction, cylinder thickness and boundary conditions are investigated on the transient temperature field of the nanocomposite cylinders.

Keywords: transient heat transfer analysis; carbon nanotubes; nanocomposite cylinders; mesh-free method; various boundary conditions

1. Introduction

Because of noticeable thermal conductivity of CNTs in comparing of other nanoparticles, CNT-reinforced composites structures have gained various applications potential. So, many researchers have been investigated on the thermal conductivity behavior of CNT/fluids or CNT/polymer because of reduction in device size and weight (Pradhan *et al.* 2009, Han and Fina 2011, Di Blasi *et al.* 2013, Di Blasi and Galgano 2013, Esfe *et al.* 2016, Kshirsagar and Shrivastava 2015, Xing *et al.* 2016). Also, addition of CNT in their matrix has been applied successfully to improve mechanical (Liu and Wang 2007, Mokashi *et al.* 2007, Zhu *et al.* 2007) and thermal (Kundalwal *et al.* 2014a, b, Kundalwal and Ray 2014) properties of CNT base nanocomposite.

Functionally graded materials (FGMs) are novel multi-phase composite materials with gradient the phase volume fractions variation in space, in specific profile(s). Transient heat transfer analysis of FGM structure had been examined in some researches. (Sladek *et al.* 2003a, b) used a meshless method based on the local boundary integral equations for analysis of transient heat conduction in FGM cylinders and finite strip. Also, they used meshless local Petrov-Galerkin method (MLPG) for the same analysis of FGM cylinders (Sladek *et al.* 2007). (Haghighi *et al.* 2009) presented a procedure for 3-D transient inverse heat conduction to estimate the unknown boundary heat flux of FGM plates.

The nonlinear thermo-elastic, vibration, and stress wave propagation behaviors of FGM cylinders are analyzed by (Shariyat *et al.* 2010) based on a third-order Hermitian finite element formulation.

About nonlinear heat conduction analysis in CNT based nanocomposite, Singh *et al.*'s work (Singh *et al.* 2007) can be mentioned. They used element free Galerkin (EFG) method and Picard and quasi-linearization schemes for nonlinear heat conduction analysis of CNTRC cylindrical representative volume element. (Imtiaz *et al.* 2016) studied on the flow and heat transfer effects of the single-walled carbon nanotubes (SWCNTs) and multi-walled carbon nanotubes (MWCNTs) with water as based fluid between two rotating and stretchable disks. They found that water based SWCNTs produce high heat transfer rate when compared with the water based MWCNTs. Moreover, some investigations are on active constrained layer damping (ACLD) of the smart laminated fuzzy fiber reinforced composite (FFRC) structures (Kundalwal *et al.* 2013, Kundalwal and Meguid 2015, Kundalwal *et al.* 2016).

To improve the reinforcement behavior of CNTs in nanocomposites and by considering of the concept of functionally graded material, the CNTs can be distributed along a certain direction as some grading patterns. So, the functionally graded carbon nanotube reinforced composites (FG-CNTRCs) are regarded as the substitute for the available functional materials (Mehtar and Panda 2016). (Shen and Xiang 2012) presented nonlinear vibrational behavior of FG-CNTRC cylindrical shells in thermal environment by considering of temperature-dependent material properties of the nanocomposite. Moreover, dynamic analysis of straight, wavy or aggregated CNT/

*Corresponding author, Associate Professor,
E-mail: g.payganeh@srttu.edu

polymer composite cylinders and plates were carried out using a moving least square (MLS) based mesh-free method (Moradi-Dastjerdi *et al.* 2013, Moradi-Dastjerdi 2016, Moradi-Dastjerdi and Momeni-Khabisi 2016, Moradi-Dastjerdi and Pourasghar 2016). Lei *et al.* (2013) presented free vibration analysis of FG-CNTRC plates in thermal environment by element-free *kp*-Ritz method. Also, based on 3-D theory of elasticity, thermo-elastic analysis of FG-CNTRC cylindrical panel is investigated (Alibeigloo 2016, Pourasghar *et al.* 2016). Finally, (Moradi-Dastjerdi *et al.* 2016, Moradi-Dastjerdi and Payganeh 2017) presented thermoelastic static and vibration analyses of FG cylinders reinforced by single-walled wavy CNTs subjected to thermal gradient and mechanical loading. They used a micro mechanical model in volume fraction form to estimate temperature-dependent mechanical properties of the nanocomposite.

It can be seen that transient heat transfer analysis of FG-CNTRC axisymmetric cylinders has not been yet considered and the present work attempts to consider transient heat transfer analysis for functionally graded CNT-reinforced nanocomposite cylinders in presence of heat flux or convection environment using a mesh-free method. In the mesh-free method, MLS shape functions are used for approximation of temperature field in the weak form of heat conduction equation for the UD and FG distribution of CNT along the radial direction and the transformation method is used for imposition of essential boundary conditions. Because of the using of the transformation method, the applied mesh-free method doesn't increase the calculations against EFG. Material properties of nanocomposite are estimated by a micro mechanical based model which used some CNT efficiency parameters. An uniformly and four linear types of FG distributions for nanotubes along the radial direction of axisymmetric cylinder are considered and the effects of cylinder thickness, thermal boundary condition and also volume fraction and distribution pattern of CNTs are investigated on transient heat transfer behavior of FG-CNTRC cylinders.

2. Material properties in FG-CNTRC cylinders

In this paper, the applied CNTRC cylinders are assumed

made from a mixture of SWCNT and an isotropic matrix. The SWCNT reinforcement is either uniformly distributed (UD) or functionally graded in the radial direction. To obtain mechanical properties of polymer nanotube composites a new rule of mixture equation assumes that the fibers have uniform dispersion in the polymer matrix. The effective material properties of the CNTRC cylinders are obtained based on a micromechanical model according to (Shen 2009)

$$k_{11} = \eta_1 V_{CN} k_{11}^{CN} + V_m k^m \tag{1}$$

$$\frac{\eta_2}{k_{22}} = \frac{V_{CN}}{k_{11}^{CN}} + \frac{V_m}{k^m} \tag{2}$$

$$c_p = V_{CN} c_p^{CN} + V_m c_p^m \tag{3}$$

$$\rho = V_{CN} \rho^{CN} + V_m \rho^m \tag{4}$$

where c_p^{CN} , ρ^{CN} and k_{ii}^{CN} are specific heat conduction, mass density, and thermal conductivity in the longitudinal ($i = 1$) and transverse ($i = 2$) directions, respectively, of the carbon nanotube. c_p^m , ρ^m and k^m are corresponding properties for the matrix. V_{CN} and V_m are the fiber (CNT) and matrix volume fractions and are related by $V_{CN} + V_m = 1$. η_j ($j=1,2$) are the CNT efficiency parameters (Shen 2009).

The profile of the variation of the fiber volume fraction has important effects on the cylinder behavior. In this paper four linear types (FG-V, FG-Λ, FG-X and FG-O) are assumed for the distribution of CNT reinforcements along the radial direction in FG-CNTRC cylinder. An UD-CNTRC cylinder with the same thickness, referred to as UD, is also considered as a comparator. These distributions

Table 1(10,10) SWCNT efficiency parameter (Shen 2009)

| V_{CN}^* | η_1 | η_2 |
|------------|----------|----------|
| 0.12 | 0.137 | 1.022 |
| 0.17 | 0.142 | 1.626 |
| 0.28 | 0.141 | 1.585 |

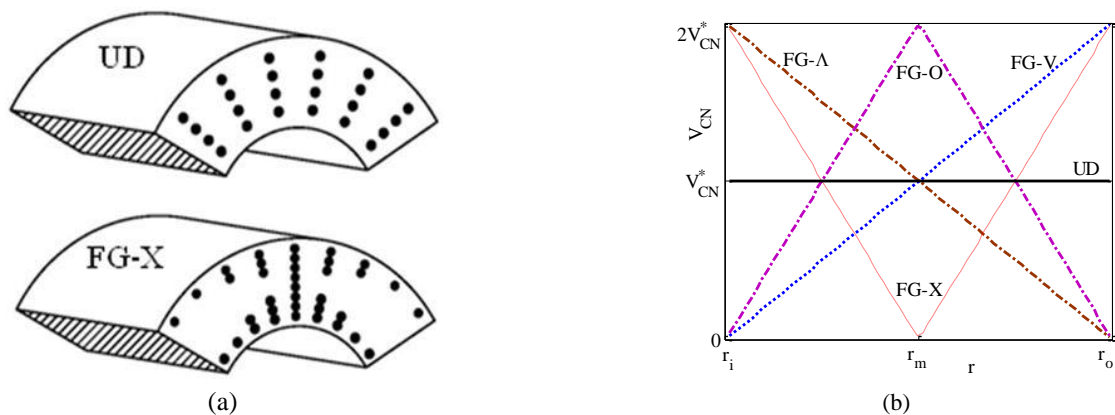


Fig. 1 (a) Schematic of CNT distributions; (b) FG-V, FG-Λ, FG-X, FG-O and UD variations of CNT volume fraction (V_{CN}) along the radial direction

along the radial direction are shown in Figs. 1 as follows

$$\text{For type V: } V_{CN} = 2\left(\frac{r-r_i}{r_o-r_i}\right)V_{CN}^* \quad (5)$$

$$\text{For type } \wedge: V_{CN} = 2\left(\frac{r_o-r}{r_o-r_i}\right)V_{CN}^* \quad (6)$$

$$\text{For type X: } V_{CN} = 4\left|\frac{r-r_m}{r_o-r_i}\right|V_{CN}^*, \quad r_m = \frac{r_i+r_o}{2} \quad (7)$$

$$\text{For type O: } V_{CN} = 2V_{CN}^* - 4\left|\frac{r-r_m}{r_o-r_i}\right|V_{CN}^*, \quad r_m = \frac{r_i+r_o}{2} \quad (8)$$

$$\text{For type UD: } V_{CN} = V_{CN}^* \quad (9)$$

where

$$V_{CN}^* = \frac{\rho^m}{\rho^m + (\rho^{CN}/w^{CN}) - \rho^{CN}} \quad (10)$$

and w^{CN} is the mass fraction of nanotube.

3. Governing equations and mesh-free numerical analysis

The transient axisymmetric heat conduction equation for FG distribution of CNT along the radial direction is taken as (Alibeigloo 2016)

$$k_r(r)\frac{\partial^2 T(r,z)}{\partial r^2} + \frac{\partial k_r(r)}{\partial r} \frac{\partial T(r,z)}{\partial r} + \frac{k_r(r)}{r} \frac{\partial T(r,z)}{\partial r} + k_z(r)\frac{\partial^2 T(r,z)}{\partial z^2} = \rho(r)c_p(r)\frac{\partial T(r,z)}{\partial t} \quad (11)$$

where $T(r, z)$ is the temperature at point $\mathbf{X} = \mathbf{X}_i(r, z)$.

In this paper, moving least square (MLS) shape functions are used for approximation of temperature vector in the weak form of heat conduction equation (Lancaster and Salkauskas 1981). Temperature vector, **temp**, can be approximated by MLS shape functions as follows

$$\mathbf{temp} = \mathbf{\Phi}\hat{\mathbf{t}} \quad (12)$$

where $\hat{\mathbf{t}}$ and $\mathbf{\Phi}$ are virtual nodal temperature vector and shape functions matrix, respectively.

$$\begin{aligned} \mathbf{temp} &= [T_1, T_2, \dots, T_n]^T, \\ \hat{\mathbf{t}} &= [\hat{T}_1, \hat{T}_2, \dots, \hat{T}_n]^T, \\ \mathbf{\Phi} &= [\Phi_1, \Phi_2, \dots, \Phi_n]^T \end{aligned} \quad (13)$$

n is the number of nodes in the support domain of the approximated point and Φ_i is MLS shape function of node located at $\mathbf{X} = \mathbf{X}_i(r, z)$ and defined as follows

$$\Phi_i(\mathbf{X}) = \underbrace{\mathbf{P}^T(\mathbf{X})[\mathbf{M}(\mathbf{X})]^{-1}w(\mathbf{X}-\mathbf{X}_i)\mathbf{P}(\mathbf{X}_i)}_{(1 \times 1)} \quad (14)$$

where, w is cubic Spline weight function, $\mathbf{P}(\mathbf{X})$ is base vector and $\mathbf{M}(\mathbf{X})$ is moment matrix. For axisymmetric problems, they are defined as

$$\mathbf{P}(\mathbf{X}) = [1, r, z]^T, \quad \mathbf{M}(\mathbf{X}) = \left[\sum_{i=1}^n w(\mathbf{X}-\mathbf{X}_i)\mathbf{P}(\mathbf{X}_i)\mathbf{P}^T(\mathbf{X}_i) \right] \quad (15)$$

By considering the approximation of Eq. (12), the weak form of heat transfer equation (Eq. (11)) is defined as (in matrix form)

$$\mathbf{C} \frac{d\hat{\mathbf{T}}}{dt} + \mathbf{K}_T \hat{\mathbf{T}} - \int_{\Gamma} \mathbf{\Phi}^T (-M_T(\mathbf{Temp}) + S) d\Gamma = 0 \quad (16)$$

Γ is a part of boundary of domain Ω with thermal flux, q , or under convection environments (natural boundary condition) where $M_T = 0$ and $S = q$, at the boundary with thermal flux and $M_T = h$ and $S = hT_{\infty}$, at the boundary under convection environments with convective heat transfer coefficient of h and ambient temperature of T_{∞} . So, the Eq. (16) can be changed as

$$\mathbf{C} \frac{d\hat{\mathbf{T}}}{dt} + \mathbf{K}_T \hat{\mathbf{T}} + \mathbf{K}_M \hat{\mathbf{T}} = \mathbf{q} \quad (17)$$

where

$$\begin{aligned} \mathbf{C} &= \int_{\Omega} (\rho c_p) \mathbf{\Phi}^T \mathbf{\Phi} dv, & \mathbf{K}_T &= \int_{\Omega} \mathbf{B}_T^T \mathbf{D}_T \mathbf{B}_T dv, \\ \mathbf{K}_M &= \int_{\Gamma} M_T \mathbf{\Phi}^T \mathbf{\Phi} dv, & \mathbf{q} &= \int_{\Gamma} q \mathbf{\Phi}^T ds \end{aligned} \quad (18)$$

$$\mathbf{Temp} = [T_1, T_2, \dots, T_N]^T, \quad \hat{\mathbf{T}} = [\hat{T}_1, \hat{T}_2, \dots, \hat{T}_N]^T \quad (19)$$

N is total number of nodes and where

$$\mathbf{B}_T = \begin{bmatrix} \frac{\partial \Phi_1}{\partial r} & \frac{\partial \Phi_2}{\partial r} & \dots & \frac{\partial \Phi_n}{\partial r} \\ \frac{\partial \Phi_1}{\partial z} & \frac{\partial \Phi_2}{\partial z} & \dots & \frac{\partial \Phi_n}{\partial z} \end{bmatrix}, \quad \mathbf{D}_T = \begin{bmatrix} k_r(r) & 0 \\ 0 & k_z(r) \end{bmatrix} \quad (20)$$

For numerical integration, problem domain is discretized to a set of background cells with gauss points inside each cell. Then global matrixes of \mathbf{C} , \mathbf{K}_T and \mathbf{K}_M are obtained numerically by sweeping all gauss points inside Ω . Similarly global flux or convection vector \mathbf{q} is formed numerically in the same manner but by sweeping all gauss points on Γ .

Imposition of essential boundary conditions (known temperature edges) in the system of Eq. (17) is not possible. Because MLS shape functions don't satisfy the Kronecker delta property. In this work transformation method is used for imposition of essential boundary conditions. For this purpose transformation matrix is formed by establishing relation between nodal temperature vector, **Temp**, and virtual temperature vector, $\hat{\mathbf{t}}$.

$$\mathbf{Temp} = \mathbf{R}\hat{\mathbf{t}} \quad (21)$$

\mathbf{R} is the transformation matrix and is defined as

$$\mathbf{R} = \begin{bmatrix} \Phi_1(\mathbf{X}_1) & \Phi_2(\mathbf{X}_1) & \dots & \Phi_N(\mathbf{X}_1) \\ \Phi_1(\mathbf{X}_2) & \Phi_2(\mathbf{X}_2) & \dots & \Phi_N(\mathbf{X}_2) \\ \vdots & \vdots & \ddots & \vdots \\ \Phi_1(\mathbf{X}_N) & \Phi_2(\mathbf{X}_N) & \dots & \Phi_N(\mathbf{X}_N) \end{bmatrix} \quad (22)$$

By using Eq. (21), system of linear Eq. (17) can be rearranged to

$$\hat{\mathbf{C}} \frac{d(\mathbf{Temp})}{dt} + \hat{\mathbf{K}}_T(\mathbf{Temp}) + \hat{\mathbf{K}}_M(\mathbf{Temp}) = \hat{\mathbf{q}} \quad (23)$$

where

$$\begin{aligned} \hat{\mathbf{C}} &= \mathbf{R}^{-T} \cdot \mathbf{C} \cdot \mathbf{R}^{-1}, & \hat{\mathbf{q}} &= \mathbf{T}^{-T} \cdot \mathbf{q} \\ \hat{\mathbf{K}}_T &= \mathbf{R}^{-T} \cdot \mathbf{K}_T \cdot \mathbf{R}^{-1}, & \hat{\mathbf{K}}_M &= \mathbf{R}^{-T} \cdot \mathbf{K}_M \cdot \mathbf{R}^{-1} \end{aligned} \quad (24)$$

Table 2 Material properties of (10,10) SWCNT and PMMA (Pourasghar *et al.* 2016, Shen 2009)

| | ρ (Kg/m ³) | c_p (j/Kg.K) | k_{11} (W/m.K) | k_{22} (W/m.K) |
|-------|-----------------------------|----------------|------------------|------------------|
| SWCNT | 1400 | 600 | 3000 | 100 |
| PMMA | 1150 | 1466 | 0.247 | 0.247 |

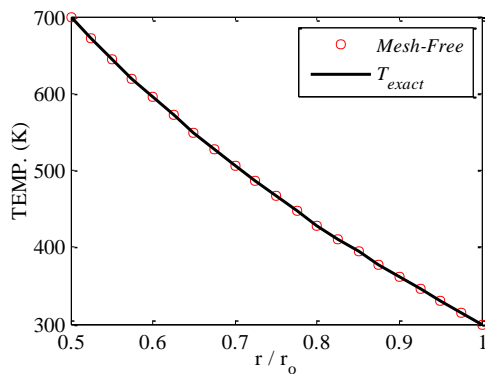


Fig. 2 Comparison of temperature distribution along the cylinder thickness

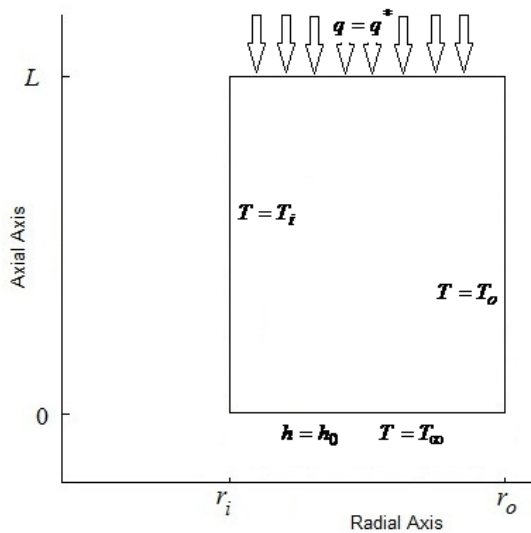
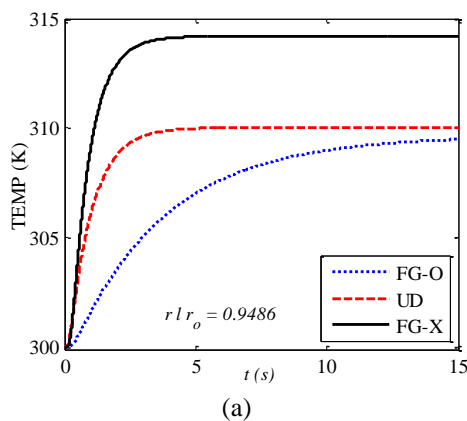


Fig. 4 Schematic figure of an axisymmetric cylinder with heat flux at top end, convection environment at bottom end, inner temperature of T_i and outer temperature of T_o

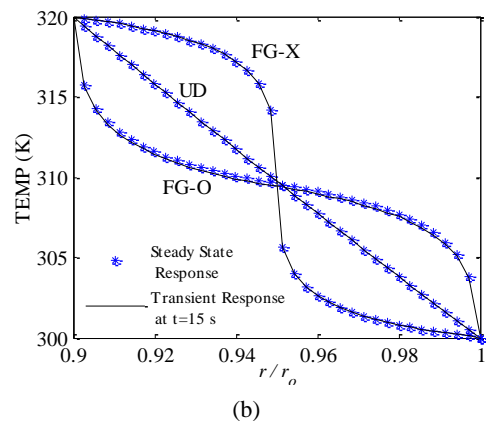


Fig. 3 Transient heat transfer responses of CNTRC cylinders with $r_i = 0.18$ m, $r_o = 0.12$ m, $L = 0.2$ m, $V_{cnv}^* = 0.17$, $T_i = 320$ K, $T_o = 300$ K and isolated ends: (a) time history of temperatures; (b) temperature along the radial direction

Now the essential boundary conditions can be enforced to the modified equations system Eq. (23) easily like the finite element method. In this work, the Newmark (forward difference) method is used for solution of Eq. (23) in time domain.

4. Results and discussions

In this section, at first the accuracy of applied method is examined. Then, effects of CNT distribution pattern and volume fraction, cylinder thickness and boundary conditions are investigated on the transient heat transfer behavior of FG-CNTRC cylinders. In the following simulations, the applied CNTRC cylinders are considered made of Poly (methyl- methacrylate, referred as PMMA) as an isotropic matrix and SWCNT as fiber. The material properties of armchair (10, 10) configuration of SWCNTs and PMMA are taken same as Table 2 (Pourasghar *et al.* 2016, Shen 2009).

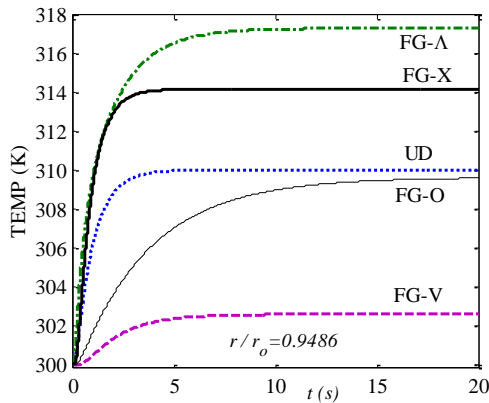
4.1 Validation models

At first, the steady state one dimensional heat transfer problem is investigated in a hollow cylinder with inside and outside temperatures of T_i and T_o , respectively. The exact solution of the problem is reported as (Hetnarski and Eslami 2009)

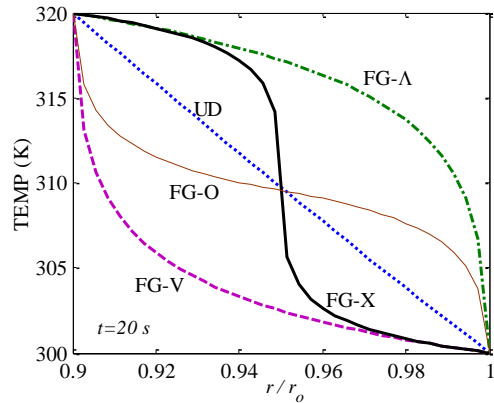
Fig. 2 shows an excellent agreement between the results of the applied mesh-free method and exact solution (Hetnarski and Eslami 2009).

$$T = \frac{T_i - T_o}{\ln(r_o - r_i)} \ln(r_o - r) + T_b \tag{25}$$

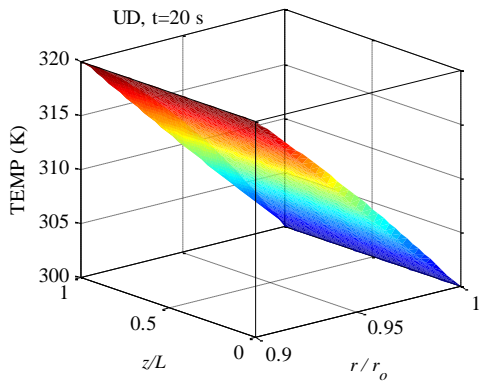
Now, consider CNTRC cylinders with inner radius of, $r_i = 0.18$ m, outer radius of, $r_o = 0.12$ m, length of, $L = 0.2$ m, CNT volume fraction of, $V_{CN}^* = 0.17$, initial temperatures, $T^0 = 300$ K, isolated top and bottom ends, inner temperature of $T_i = 320$ K and outer temperature of $T_o = 300$ K. Fig. 3(a) shows time histories of temperatures of the UD, X and O-CNTRC cylinders at $r/r_o = 0.9486$. It's observed UD and X cylinders get stationary condition before $t = 5$ s while O-type cylinder gets steady state after $t = 15$ s. Fig. 3(b) compares the steady state results of the cylinders and transient responses of them at $t = 15$ s. It can be seen that UD and X cylinders has the same results in both cases of steady state condition and transient at $t = 15$ s, but in O-



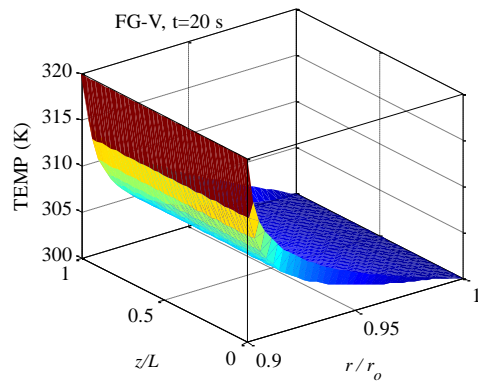
(a)



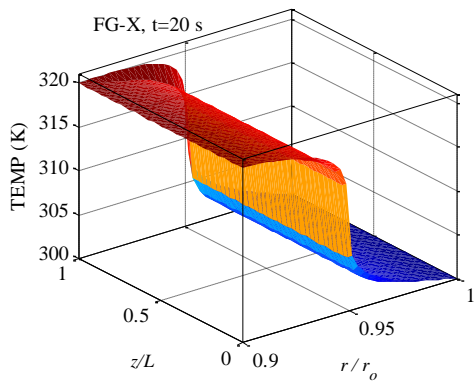
(b)



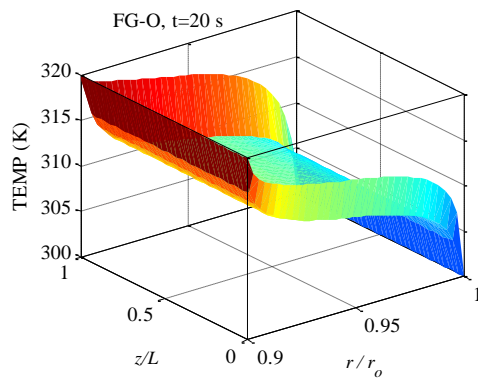
(c)



(d)



(e)



(f)

Fig. 5 Transient heat transfer responses of first model CNTRC cylinders: (a) time history of temperatures; (b) temperature along the radial direction; (c) temperature distribution of UD type; (d) temperature distribution of V type; (e) temperature distribution of X type (f) temperature distribution of O type

CNTRC cylinder, the temperature transient condition at $t = 15$ s is a little less than steady state results.

4.2 Transient heat transfer in FG-CNTRC cylinders

After validation of the applied mesh-free method, transient heat transfer analysis of FG-CNTRC cylinders with various boundary conditions is investigated. At first model, consider CNTRC cylinders with $r_i = 0.18$ m, $r_o = 0.12$ m, $L = 0.2$ m, $V_{CN}^* = 0.17$, initial temperatures, $T^0 = 300$ K. In these cylinders, $T_i = 320$ K, $T_o = 300$ K, top end is under heat flux of $q_u = 10$ kW/m² and bottom end is under

environment with heat transfer by convection of $h = 100$ W/m²K and $T_\infty = 350$ K (See Fig. 4). Fig. 5 shows the transient heat transfer results of the UD and FG-CNTRC cylinders. Fig. 5(a) illustrates temperatures of the CNTRC cylinders (at radius of $r_i/r_o = 0.9486$ and mid length) get steady state condition.

It can be seen that X-CNTRC cylinders, because of the high value of CNT volume fraction in the surfaces and the high value of CNT thermal conductivity, has the maximum speed of convergency while O-CNTRC cylinder has the minimum one. Fig. 5(b) reveals that distribution of CNTs, because of the higher value of CNT thermal conductivity

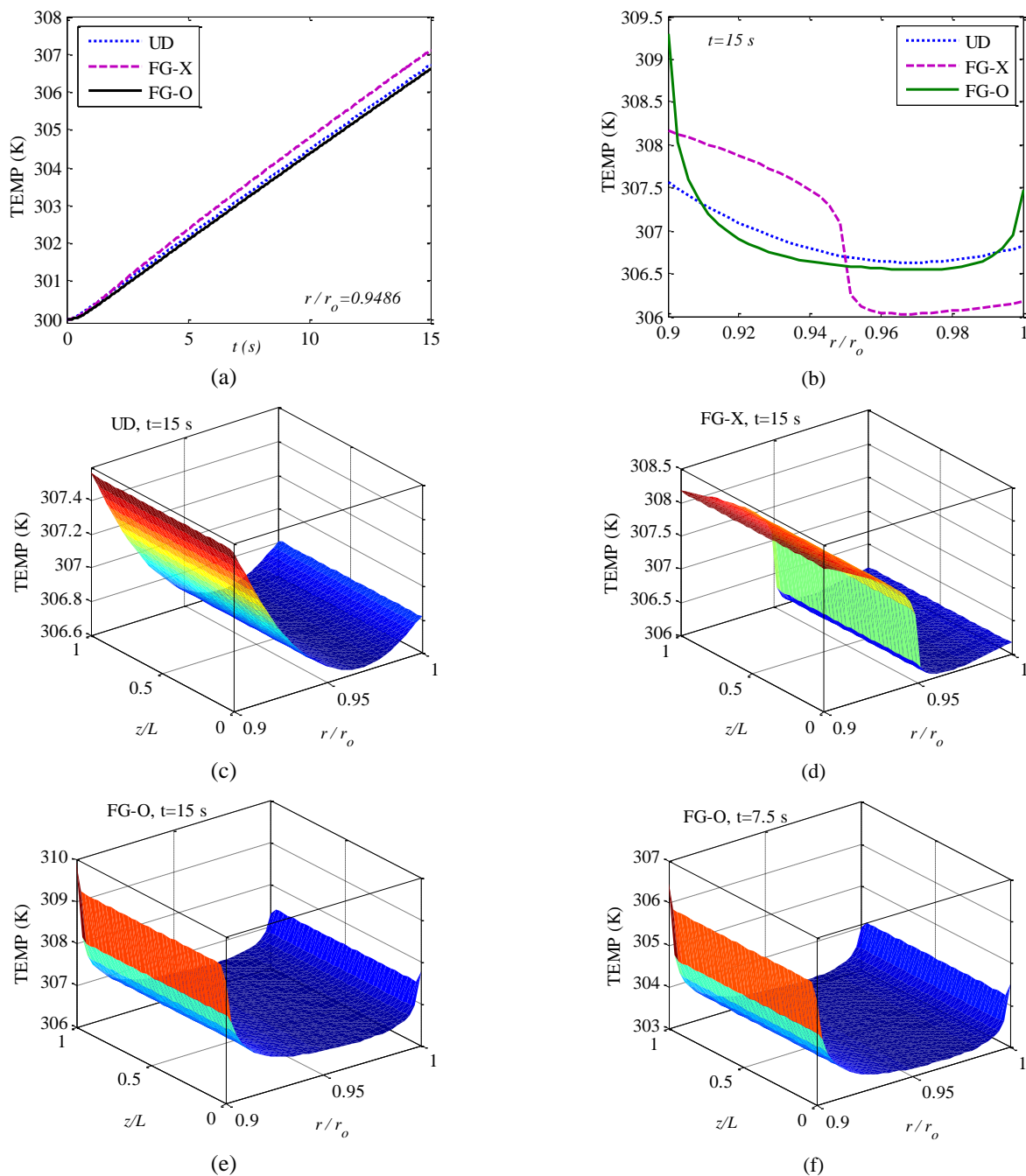


Fig. 6 Transient heat transfer responses of second model CNTRC cylinders: (a) time history of temperatures: (b) temperature along the radial direction; (c) temperature distribution of UD type; (d) temperature distribution of X type; (e) temperature distribution of O type; (f) temperature distribution of O type at $t = 7.5$ s

than PMMA, has an important effect on the temperature distribution of the CNTRC cylinders at $t = 20$ s. FG- \wedge and FG-V types of CNTRC cylinders have the biggest and smallest mid values of cylinder temperatures, respectively. So, \wedge type cylinder has the best conductivity condition. Figs 5(c)-(f) show temperature distributions of the UD, V, X and O types of CNTRC cylinders at $t = 20$ s, respectively. It can be seen that the effect of heat flux and convection environment in O-CNTRC cylinder is more than the other types of cylinders.

For second model, reconsider the previous CNTRC cylinders with boundary conditions of outer convection environment of $h = 100$ W/m²K and $T_\infty = 350$ K, inner heat flux of $q_i = 10$ kW/m² and isolated ends. Fig. 6 shows responses of transient heat transfer of CNTRC cylinders. Fig. 6(a) illustrates the cylinders don't get steady state condition in first 15 seconds. Fig. 6(b) reveals that the temperatures of inner radius of the cylinders are more than outer ones, so effect of the applied flux condition on temperature transfer is more than the convection condition. Also, O-CNTRC cylinder has the biggest values of inner and outer temperatures and UD cylinder has a smooth temperature variation along radial direction at $t = 15$ s. These temperature distributions are obtained because of the

kind of CNT distributions and the high value of CNT thermal conductivity. Figs. 6(c)-(e) illustrated temperature distributions of UD, X and O types of cylinders at $t = 15$ s. It can be seen that temperatures have no variation along the axial direction because of the isolated ends. Fig 6(f) shows temperature distribution of O-CNTRC cylinders at $t = 7.5$ s. Comparing the results at two reported times shows that temperature of the cylinder is raised by passing time.

The effect of CNT volume fraction is examined in third model. So, consider O-CNTRC cylinders with $r_i = 0.18$ m, $r_o = 0.2$ m, $L = 0.2$ m, initial temperatures of $T^0 = 300$ K and with the boundary conditions as the second model. Fig. 7(a) shows the temperatures of cylinders are increased by passing time and the cylinders don't have stationary condition before $t = 15$ s. Fig. 7(b) reveals that increasing of CNT volume fraction decreases temperatures around inner radius but increases temperatures in remain areas.

Finally, reconsider the second model but with $r_i = 0.16$ m as forth model. Fig. 8(a) shows time history of temperature in the cylinders. A time delay about 2 seconds can be seen in the temperatures rising of the thicker cylinders. Also, the stationary condition cannot be seen until $t = 15$ s. By comparing between Figs. 6(b) and 8(b), it can be seen that the temperatures of the thicker cylinders are

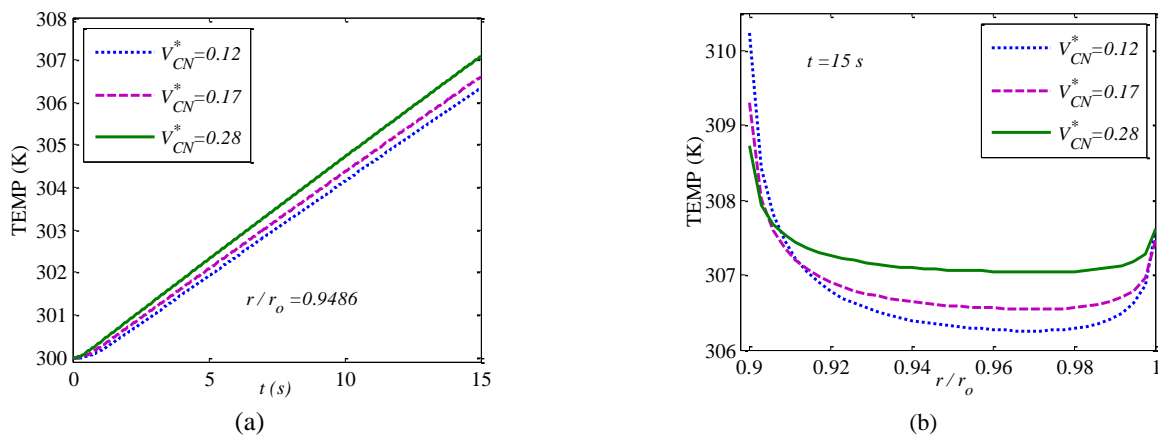


Fig. 7 Transient heat transfer responses of third model CNTRC cylinders: (a) time history of temperatures; (b) temperature along the radial direction

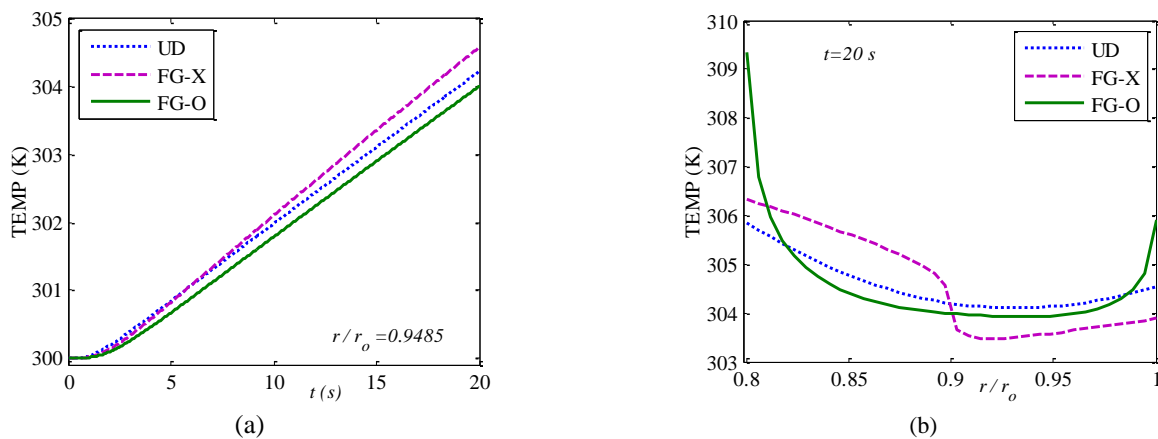


Fig. 8 Transient heat transfer responses of forth model CNTRC cylinders: (a) time history of temperatures; (b) temperature along the radial direction

less than thinner ones even passing 20 seconds except inner temperature of O-CNTRC.

5. Conclusions

In this work, transient heat transfer behaviors of functionally graded CNT reinforced cylinders with various essential (known temperature) and natural (heat flux or convection environment) boundary conditions were investigated by an MLS based mesh-free method. The nanocomposite material properties were assumed functionally graded along the radius and estimated by a micro mechanical based model. The effects of CNT distribution pattern and volume fraction, cylinder thickness and boundary conditions were investigated on the transient temperature field of the nanocomposite cylinders and following results were obtained from this analysis:

- The developed mesh-free method has an excellent accuracy and convergency on transient heat transfer analysis of the FG-CNTRC cylinders.
- The distribution of CNTs has an important effect on the temperature distribution and convergency speed of the CNTRC cylinders
- \wedge and \vee types of CNTRC cylinders have the best and worse conductivity conditions, respectively.
- Increasing of CNT volume fraction decreases temperatures around inner radius but increases temperatures in remain areas.
- The temperatures of the thicker cylinders are less than thinner ones even passing more times, except inner temperature of O-CNTRC.

References

- Alibeigloo, A. (2016), "Elasticity solution of functionally graded carbon nanotube-reinforced composite cylindrical panel subjected to thermo mechanical load", *Compos. Part B*, **87**, 214-226. Available from: <http://dx.doi.org/10.1016/j.compositesb.2015.09.060>
- Di Blasi, C. and Galgano, A. (2013), "Influences of properties and heating characteristics on the thermal decomposition of polymer/carbon nanotube nanocomposites", *Fire Safety J.*, **59**, 166-177.
- Di Blasi, C., Galgano, A. and Branca, C. (2013), "Modeling the thermal degradation of poly (methyl methacrylate)/carbon nanotube nanocomposites", *Polym. Degrad. Stabil.*, **98**(1), 266-275.
- Esfe, M.H., Motahari, K., Sanatizadeh, E., Afrand, M., Rostamian, H. and Ahangar, M.R.H. (2016), "Estimation of thermal conductivity of CNTs-water in low temperature by artificial neural network and correlation", *Int. Commun. Heat Mass Transfer*, **76**, 376-381. Available from: <http://dx.doi.org/10.1016/j.icheatmasstransfer.2015.12.012>
- Haghighi, M.G., Eghtesad, M., Malekzadeh, P. and Neculescu, D.S. (2009), "Three-dimensional inverse transient heat transfer analysis of thick functionally graded plates", *Energy Convers. Manag.*, **50**(3): 450-457. Available from: <http://dx.doi.org/10.1016/j.enconman.2008.11.006>
- Han, Z. and Fina, A. (2011), "Thermal conductivity of carbon nanotubes and their polymer nanocomposites: A review", *Progress Polym. Sci.*, **36**(7), 914-944.
- Hetnarski, R.B. and Eslami, M.R. (2009), *Thermal Stresses—Advanced Theory and Applications*, Springer, The Netherlands.
- Imtiaz, M., Hayat, T., Alsaedi, A. and Ahmad, B. (2016), "Convective flow of carbon nanotubes between rotating stretchable disks with thermal radiation effects", *Int. J. Heat Mass Transfer*, **101**, 948-957. Available from: <http://dx.doi.org/10.1016/j.ijheatmasstransfer.2016.05.114>
- Kshirsagar, J.M. and Shrivastava, R. (2015), "Review of the influence of nanoparticles on thermal conductivity, nucleate pool boiling and critical heat flux", *Heat Mass Transfer*, **51**(3), 381-398.
- Kundalwal, S.I. and Meguid, S.A. (2015), "Effect of carbon nanotube waviness on active damping of laminated hybrid composite shells", *Acta Mechanica*, **226**(6), 2035-2052.
- Kundalwal, S.I. and Ray, M.C. (2014), "Estimation of thermal conductivities of a novel fuzzy fiber reinforced composite", *Int. J. Thermal Sci.*, **76**, 90-100.
- Kundalwal, S.I., Kumar, R.S. and Ray, M.C. (2013), "Smart damping of laminated fuzzy fiber reinforced composite shells using 1–3 piezoelectric composites", *Smart Mater. Struct.*, **22**(10), p. 105001.
- Kundalwal, S.I., Kumar, R.S. and Ray, M.C. (2014a), "Effective thermal conductivities of a novel fuzzy carbon fiber heat exchanger containing wavy carbon nanotubes", *Int. J. Heat Mass Transfer*, **72**, 440-451.
- Kundalwal, S.I., Kumar, R.S. and Ray, M.C. (2014b), "Effective thermal conductivities of a novel fuzzy fiber-reinforced composite containing wavy carbon nanotubes", *J. Heat Transfer*, **137**(1), p. 012401.
- Kundalwal, S.I., Kumar, R.S. and Ray, M.C. (2016), "Smart damping of laminated fuzzy fiber reinforced composite shells using 1–3 piezoelectric composites", *J. Vib. Control*, **22**(6), 1526-1546. Available from: <http://stacks.iop.org/0964-1726/22/i=10/a=105001?key=crossref.7fe9133a96d0b74e04e872cc0f6acbe2>
- Lancaster, P. and Salkauskas, K. (1981), "Surfaces generated by moving least squares methods", *Math. Computat.*, **37**(155), 141-158.
- Lei, Z.X., Liew, K.M. and Yu, J.L. (2013), "Free vibration analysis of functionally graded carbon nanotube-reinforced composite plates using the element-free *kp*-Ritz method in thermal environment", *Compos. Struct.*, **106**, 128-138.
- Liu, T.T. and Wang, X. (2007), "Dynamic elastic modulus of single-walled carbon nanotubes in different thermal environments", *Phys. Lett. A*, **365**(1), 144-148.
- Mehar, K. and Panda, S.K. (2016), "Geometrical nonlinear free vibration analysis of FG-CNT reinforced composite flat panel under uniform thermal field", *Compos. Struct.*, **143**, 336-346. Available from: <http://dx.doi.org/10.1016/j.compstruct.2016.02.038>
- Mokashi, V.V., Qian, D. and Liu, Y. (2007), "A study on the tensile response and fracture in carbon nanotube-based composites using molecular mechanics", *Compos. Sci. Technol.*, **67**(3), 530-540.
- Moradi-Dastjerdi, R. (2016), "Wave propagation in functionally graded composite cylinders reinforced by aggregated carbon nanotube", *Struct. Eng. Mech., Int. J.*, **57**(3), 441-456.
- Moradi-Dastjerdi, R. and Momeni-Khabisi, H. (2016), "Dynamic analysis of functionally graded nanocomposite plates reinforced by wavy carbon nanotube", *Steel Compos. Struct., Int. J.*, **22**(2), 277-299.
- Moradi-Dastjerdi, R. and Pourasghar, A. (2016), "Dynamic analysis of functionally graded nanocomposite cylinders reinforced by wavy carbon nanotube under an impact load", *J. Vib. Control*, **22**(4), 1062-1075.
- Moradi-Dastjerdi, R. and Payganeh, G. (2017), "Thermoelastic Vibration Analysis of Functionally Graded Wavy Carbon Nanotube-Reinforced Cylinders", *Polym. Compos.* DOI: 10.1002/pc.24278
- Moradi-Dastjerdi, R., Foroutan, M. and Pourasghar, A. (2013),

- “Dynamic analysis of functionally graded nanocomposite cylinders reinforced by carbon nanotube by a mesh-free method”, *Mater. Des.*, **44**, 256-266. Available from: <http://dx.doi.org/10.1016/j.matdes.2012.07.069>
- Moradi-Dastjerdi, R., Payganeh, G. and Tajdari, M. (2016), “Thermoelastic analysis of functionally graded cylinders reinforced by wavy CNT using a mesh-free method”, *Polym. Compos.* DOI: 10.1002/pc.24183
- Pourasghar, A., Moradi-Dastjerdi, R., Yas, M.H., Ghorbanpour Arani, A. and Kamarian, S. (2016), “Three-dimensional analysis of carbon nanotube-reinforced cylindrical shells with temperature-dependent properties under thermal environment”, *Polym. Compos.* DOI: 10.1002/pc.24046
- Pradhan, N.R., Duan, H., Liang, J. and Iannacchione, G.S. (2009), “The specific heat and effective thermal conductivity of composites containing single-wall and multi-wall carbon nanotubes”, *Nanotechnology*, **20**(24), p. 245705.
- Shariyat, M., Khaghani, M. and Lavasani, S.M.H. (2010), “Nonlinear thermoelasticity, vibration, and stress wave propagation analyses of thick FGM cylinders with temperature-dependent material properties”, *Eur. J. Mech. / A Solids*, **29**(3), 378-391. Available from: <http://dx.doi.org/10.1016/j.euromechsol.2009.10.007>
- Shen, H.S. (2009), “Nonlinear bending of functionally graded carbon nanotube-reinforced composite plates in thermal environments”, *Compos. Struct.*, **91**(1), 9-19. Available from: <http://dx.doi.org/10.1016/j.compstruct.2009.04.026>
- Shen, H.S. and Xiang, Y. (2012), “Nonlinear vibration of nanotube-reinforced composite cylindrical shells in thermal environments”, *Comput. Methods Appl. Mech. Eng.*, **213**, 196-205.
Available from: <http://dx.doi.org/10.1016/j.cma.2011.11.025>
- Singh, I.V., Tanaka, M. and Endo, M. (2007), “Meshless method for nonlinear heat conduction analysis of nano-composites”, *Heat Mass Transfer*, **43**(10), 1097-1106.
- Sladek, J., Sladek, V., Krivacek, J. and Zhang, C. (2003a), “Local BIEM for transient heat conduction analysis in 3-D axisymmetric functionally graded solids”, *Computat. Mech.*, **32**(3), 169-176.
- Sladek, J., Sladek, V. and Zhang, C. (2003b), “Transient heat conduction analysis in functionally graded materials by the meshless local boundary integral equation method”, *Computat. Mater. Sci.*, **28**(3), 494-504.
- Sladek, J., Sladek, V., Hellmich, C. and Eberhardsteiner, J. (2007), “Heat conduction analysis of 3-D axisymmetric and anisotropic FGM bodies by meshless local Petrov–Galerkin method”, *Computat. Mech.*, **39**(3), 323-333.
- Xing, M., Yu, J. and Wang, R. (2016), “Experimental investigation and modelling on the thermal conductivity of CNTs based nanofluids”, *Int. J. Thermal Sci.*, **104**, 404-411. Available from: <http://dx.doi.org/10.1016/j.ijthermalsci.2016.01.024>
- Zhu, R., Pan, E. and Roy, A. (2007), “Molecular dynamics study of the stress–strain behavior of carbon-nanotube reinforced Epon 862 composites”, *Mater. Sci. Eng. A*, **447**(1), 51-57.